JOURNAL OF MATERIALS SCIENCE 24 (1989) 425–431

Temperature-programmed reduction of Ni–Mo oxides

JOAQUÍN L. BRITO, JORGE LAINE
Centro de Química, Instituto Venezolano de Investigaciones Científicas, Apartado 21827, Caracas 1020-A, Venezuela

KERRY C. PRATT
CSIRO Division of Materials Science, University of Melbourne, Parksville, Victoria 3052, Australia

Temperature-programmed reduction (TPR) has been employed to study Ni–Mo mixed oxides which were previously used as model hydrodesulphurization (HDS) catalysts, using compositions ranging from pure MoO_3 to pure NiO. An assignment of TPR signals to the different bulk phases was attempted. Good agreement between TPR spectra and structural data obtained previously from X-ray and electron diffraction was observed. TPR traces were consistent with proposed mechanisms of reduction of the bulk oxides MoO_3, MoO_2, NiO and $NiMoO_4$. The variations in TPR spectra were interpreted in terms of effects such as crystallite size, ageing of the samples, hydrous state and chemical interactions between the different species. The significance of these reducibility results for HDS catalysis is discussed.

1. Introduction

Molybdenum-based oxides and sulphides are versatile catalysts for some reactions of industrial importance. In particular, nickel–molybdenum mixed oxides are effective catalysts for reactions such as carbon monoxide methanation [1], partial oxidation of hydrocarbons [2, 3] and petroleum hydrodesulphurization (HDS) [4].

Generally, the oxidic precursor of these catalysts is activated before reaction by means of reductive pretreatments (e.g. reduction with H_2 or sulphiding with H_2S), as long as the catalytic active form may involve a mean oxidation state lower than that of the most stable oxide. On the other hand, the structural characteristics of the starting material may determine the steady-state activity and selectivity of the working catalyst. Thus, a study of the reducibility of structurally well characterized precursors should provide useful information regarding the active form of the catalyst.

Among procedures to study catalyst reducibility, temperature-programmed reduction (TPR) [5] is a characterization technique which has been recently developed in the study of an ample range of catalyst materials: e.g. amorphous co-precipitated oxides [6] and supported, very dispersed noble-metal catalysts [5]. It allows one to study the reducibility of solid samples under dynamic conditions by continuously monitoring the consumption of a reducing gas (e.g. H_2 or CO) while a known heating programme (generally a linear one) is being performed on the sample.

In a previous publication [7] TPR spectra of Ni–Mo oxides supported in various porous oxides were reported, and their possible connection to catalytic HDS activity was discussed. It is felt that a more comprehensive characterization study of this catalytic system requires reducibility measurements of the unsupported oxides. Therefore, the present work has been focused to study the TPR of several co-precipitated Ni–Mo oxides, some of which have previously been used as model HDS catalysts [8, 9].

2. Experimental methods

2.1. Materials

The same series of Ni–Mo mixed oxides (Series 1) prepared for a previous work [9] using a method of continuous co-precipitation was employed. The samples had compositions ranging from pure MoO_3 to pure NiO. The structural characteristics of the freshly prepared oxides, as determined by X-ray diffraction (XRD) and electron diffraction, have been published elsewhere [10]. As the present characterization has been performed a considerable time after preparation, the samples were fully characterized again by XRD and chemical analysis, as described below. Table I presents the composition and colour of the samples.

Another group of Ni–Mo oxides (Series 2) were prepared by a static co-precipitation technique, essentially as described by Corbet *et al.* [11]. Details of the preparation are given in Table I, along with other characteristics of the oxides.

Samples of pure oxides used as standards included MoO_3 (BDH analytical reagent) and NiO (BDH laboratory reagent). MoO_2 was prepared by low-temperature reduction of the commercial MoO_3 with H_2. The structure of the final product was confirmed by XRD.

2.2. Physico-chemical characterization

Chemical analysis of the mixed oxides was carried out

0022–2461/89 $03.00 + .12 © *1989 Chapman and Hall Ltd.*

TABLE I Characteristics of the oxides

Series	Sample	r*	Preparation†	Colour
1	A	0	CC	Pale green
	B	0.30	CC	Olive green
	C	0.41	CC	Greyish-green
	D	0.55	CC	Golden yellow
	E	0.73	CC	Black
	F	0.79	CC	Black
	G	0.92	CC	Black
	J	1	CC	Greenish-grey
2	U	0.51	SC, pH5; NC	Golden yellow
	V	0.45	SC, pH8; NC	Green
	W	0.43	SC, pH7; C at 500° C	Green
	X	0.44	SC, pH7; C at 600° C	Green
Standards	MoO_3	0	COM	White
	MoO_2	0	Reduction of COM MoO_3	Black
	NiO	1	COM	Black

*Atomic fraction, r = Ni/(Ni + Mo).
†CC, continuous co-precipitation [9]; SC, static co-precipitation (as in [11]) at pH indicated; NC, not calcined (only dried at 120° C); C, calcined at temperature indicated, after drying; COM, commercial sample.

by atomic absorption with a Varian GTA-95 apparatus. The composition is reported (Table I) in terms of the atomic ratio r = Ni/(Ni + Mo).

XRD diagrams of the samples were recorded by means of a Philips PW 1730 instrument, using Cu$K\alpha$ radiation and a nickel filter.

Thermogravimetric analysis (TGA) of some samples was carried out using a Cahn 2000 Electrobalance and a TGA Fisher Accessory. Heating was performed at 20° C min^{-1} between 25 and 500° C under flowing helium (100 ml min^{-1}).

Scanning electron microscopy (SEM) observation of selected samples was performed with a Philips PSEM 500 instrument.

2.3. Temperature-programmed reduction

The apparatus for TPR measurements has been described previously [7]. It consists of a continuous-flow system with electronic mass flow controllers (Matheson 8240). A mixture of hydrogen (10 ml min^{-1}) and nitrogen (40 ml min^{-1}), purified with deoxygenation and molecular sieves traps, flows through the 5 mg sample bed, poured on a frit in a quartz reactor. A liquid nitrogen trap set before the thermal conductivity detector allows removal of the last traces of moisture from the gaseous current; another trap set after the reactor removes the water produced during reduction. Thus, the detector response is only proportional to the H_2 consumption. Heating (20° C min^{-1}) of the quartz reactor between 25 and 910° C is performed with a tubular furnace connected to a Eurotherm 070 controller and a Eurotherm 125 programmer.

Quantification of the amount of H_2 consumed in the runs was carried out by a peak area integration method; the detector response was calibrated by injection of a known volume of H_2. The results agreed within 10% with the theoretical predictions.

3. Results and discussion

3.1. X-ray diffraction

XRD diagrams of the continuously co-precipitated oxides (Series 1) and of commercial samples are shown in Figs 1 and 2. In general these results agree with the previously reported structural studies of unsupported Ni–Mo oxide catalysts [10, 12]. However, it should be noted that the XRD traces of Samples E and F are very broad, suggesting highly amorphous structures. By means of electron diffraction it was shown that the only crystalline phase present was NiO, molybdenum oxides being undetectable [10]. Also, Sample D did not show the line at d = 0.3336 nm reported in the previous work for the same sample [10]. This line is

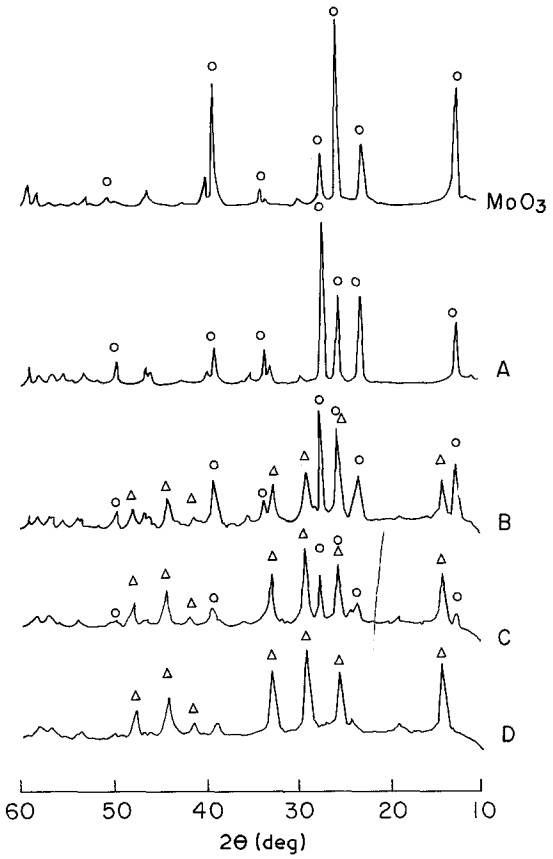

Figure 1 X-ray diffraction diagrams of commercial MoO_3 and of molybdenum-rich samples of Series 1: (○) MoO_3 (orthorhombic), (△) α-$NiMoO_4$.

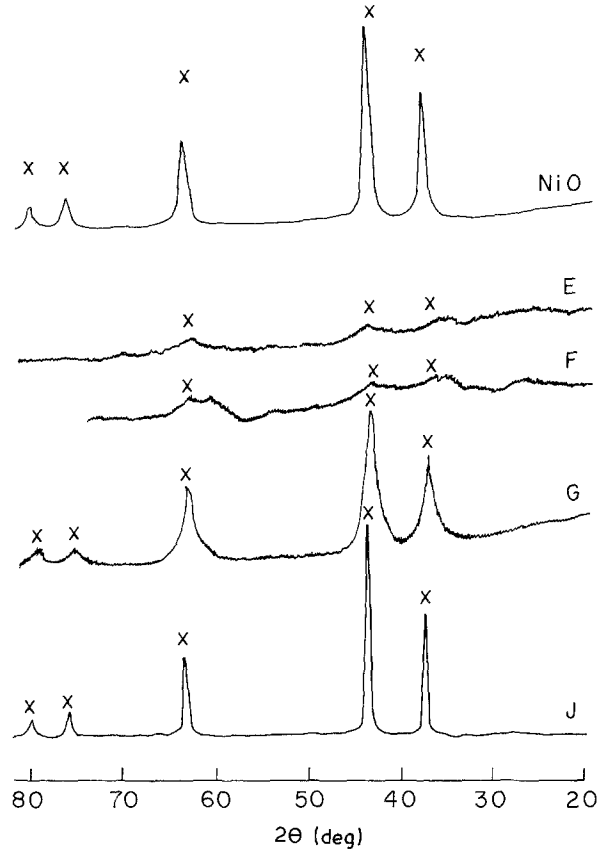

Figure 2 X-ray diffraction diagrams of commercial NiO and of nickel-rich samples of Series 1: (×) NiO.

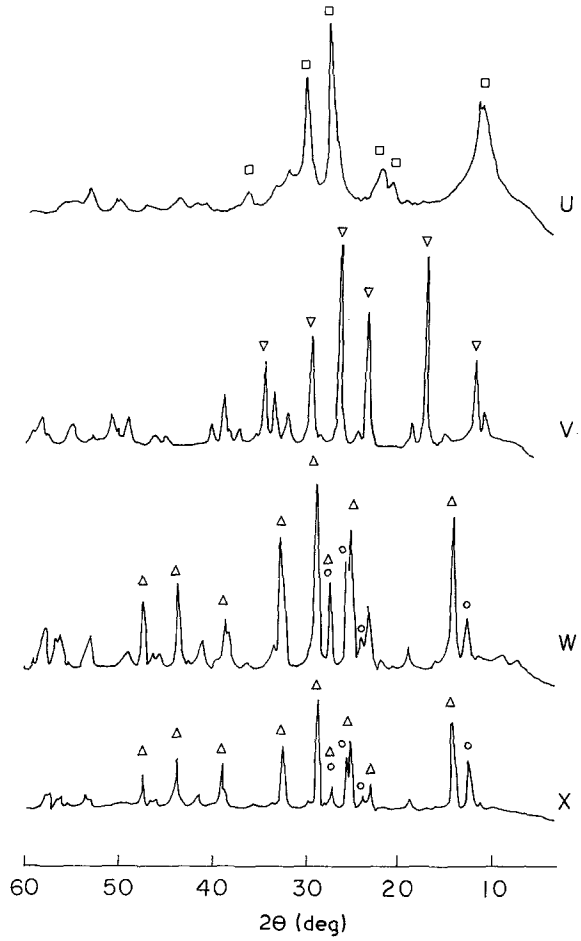

Figure 3 X-ray diffraction diagrams of samples of Series 2: (○, △) as in Fig. 1; (□) $NiMoO_4 \cdot xH_2O$; (▽) $xNiO \cdot MoO_3 \cdot yH_2O$.

characteristic of β-$NiMoO_4$ that probably was present in the freshly prepared sample stabilized by a slight excess of NiO [2, 13], but which should have been transformed to the thermodynamically more stable α-$NiMoO_4$ due to ageing.

Another difference regards the greenish-grey colour of Sample J ($r = 1$). The colour reported previously was black [9], which is also the colour of the standard NiO available. However, the XRD traces of both Sample J and the standard show good agreement (Fig. 2).

Fig. 3 presents XRD traces of the Series 2 oxides. Samples W and X show good coincidence, and suggest the presence of a mixture of α-$NiMoO_4$ and MoO_3, in agreement with the slight excess of molybdenum over nickel in these samples ($r \sim 0.44$). Conversely, no MoO_3 peaks can be appreciated in the XRD diagram of Sample V ($r = 0.45$), which corresponds to the phase $xNiO \cdot MoO_3 \cdot yH_2O$. Sample U is consistent with the diffraction reported for $NiMoO_4 \cdot x\ H_2O$ [12].

It should be noted that the intensities of the lines of the commercial sample of MoO_3 and of Sample A are widely different, although all the lines of both traces correspond to orthorhombic MoO_3 (Fig. 1). In agreement with a recent report of Bruckman *et al.* [14], the higher crystallinity of the commercial sample may be assigned to a preferential orientation in crystal growth in the direction of the (0 1 0) plane. This preferential orientation of the crystallites was further confirmed by direct microscopic observation (Fig. 4).

TABLE II Quantitative TPR data of selected samples

Sample	1st peak (mmol H_2)	2nd peak (mmol H_2)	Ratio of peaks*
Commercial MoO_3	0.036	0.071	1.97
A	0.039	0.073	1.87
D	0.074	0.017	4.35
U	0.063	0.019	3.32
V	0.056	0.020	2.80
W	0.067	0.025	2.68
X	0.067	0.025†	2.68
J	0.067	–	–

*Ratio of larger to smaller peak.
†Composite of the two high T_m peaks, at 730 and 770° C.

3.2. Thermal analysis

Fig. 5 presents TGA runs of the Series 2 oxides. When compared with the data of Corbet *et al.* [11], they confirm the XRD results: Samples U and V are both hydrated oxides, the first one behaving as $NiMoO_4 \cdot xH_2O$, whereas the second one has a thermogram characteristic of $xNiO \cdot MoO_3 \cdot yH_2O$.

3.3. Temperature-programmed reduction

3.3.1. General observations

TPR spectra are shown in Figs 6 and 7. In each case the T_m value (defined as the temperature of maximum H_2 consumption, i.e. the maximum of the peak) is displayed beside the corresponding TPR signal. Table II shows quantitative data derived from Fig. 6 for those samples where there is a clear separation of the peaks.

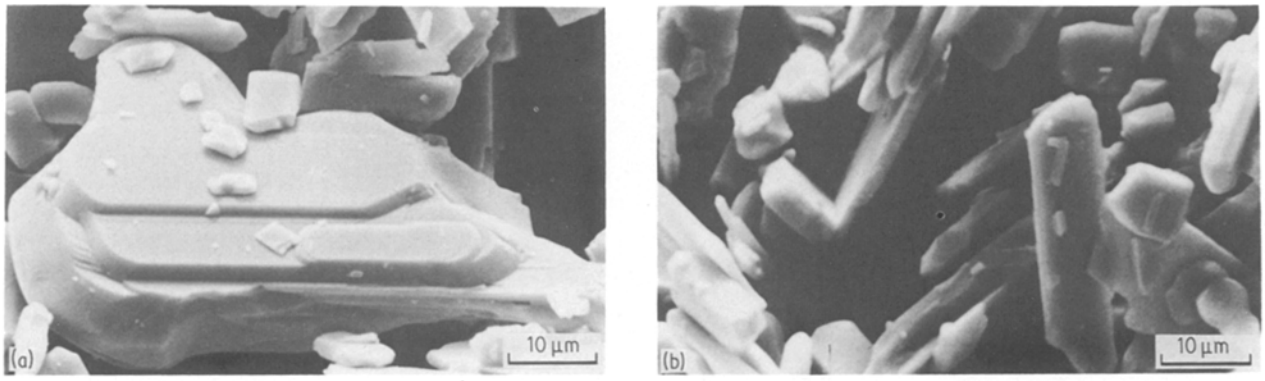

Figure 4 Scanning electron micrographs of (a) commercial MoO_3, (b) Sample A.

In general samples with similar composition show similar spectra. For example, Sample A and commercial MoO_3 show two peaks with similar ratio of sizes and T_m values; NiO and Sample J have very symmetric peaks at low T_m; samples consisting of diverse $NiMoO_4$ phases (C, D, U, V, W and X) show two main peaks around 500 and 700° C.

It can be seen (Fig. 7) that molybdenum-containing oxides are less easily reduced than pure NiO (see also the standards in Fig. 6a). However, increasing amounts of molybdenum in the nickel-rich samples (up to 27 at %) have only a slight influence on the reducibility of the resulting oxides (Samples E to G, Fig. 7). This result is in line with XRD (Fig. 2) and electron diffraction [10] data, which were not able to show any other crystalline phase but NiO.

The MoO_2 standard (aged several months) was sensitive to heat treatments applied before TPR (Fig. 6b). The low T_m peak tended to disappear with increasing severity of pretreatment under flowing helium. These results suggest that exposure to O_2, even at room temperature, leads to the formation of a very thin oxidized layer in this sample. In accordance with this proposal, the bulk of the aged sample remains unaffected, as found by XRD, and the freshly prepared MoO_2 showed only the high T_m peak (Fig. 6a).

3.3.2. Samples without nickel ($r = 0$)

Generally, TPR spectra of both MoO_3 samples show good agreement in shape and T_m values. The first and second TPR signals could be assigned, respectively, to the two steps of the mechanism of reduction:

$$MoO_3 + H_2 \rightarrow MoO_2 + H_2O$$

$$MoO_2 + 2H_2 \rightarrow Mo + 2H_2O$$

The shoulder in the low-temperature side of the first peak confirms that reduction of MoO_3 starts at low temperatures (about 400° C in these conditions), in agreement with previous workers [15, 16]. The assignment of the peaks is reinforced by the fact that the ratio of area of the second to the first peak is about 2 (Table II), confirming that the second step consumes twice as much H_2 as the first one.

Similar TPR spectra have been reported by Thomas *et al.* [17] and by Arnoldy *et al.* [16]. In the first work, XRD analysis was performed after interruption of the TPR runs at selected temperatures. In agreement with the mechanism postulated above, MoO_2 was detected just after the first peak, whereas Mo_4O_{11} proved to be present after the low T_m shoulder. This latter result may be accounted for by a mechanism of reduction from MoO_3 to MoO_2 through non-stoichiometric oxides, as indicated elsewhere [18, 19].

The small differences in T_m value of the two MoO_3 samples (Figs 6a and 7a) may be explained by the higher crystallinity of the commercial sample (Fig. 4). This latter has large crystals of high exposure of their basal (0 1 0) plane, whereas Sample A contains smaller particles. Accordingly, the peaks of the commercial MoO_3 appear at T_m values 10 to 15° C lower than those of Sample A, because the slower step in the reduction of MoO_3 is probably the diffusion of oxygen ions (or of the water product) through the shear structure of this compound [19]. Also in this line is the observation of an even lower T_m for the first peak of aged MoO_2 samples.

Attention should be given to the fact that the main peak of the MoO_2 standard has a T_m considerably higher than the second peak of MoO_3. It may be speculated that the reduction of MoO_3 to MoO_2 under the dynamic conditions of TPR proceeds with formation of a very amorphous or "porous" [16] oxide. This material is more easily reduced than the crystalline MoO_2 prepared by low-temperature (static) reduction of MoO_3, which suffered long reduction and annealing times. Also, pure MoO_2 is known to have cluster characteristics [20], i.e. Mo–Mo bond-like interaction, that may make it more resistant to reduction.

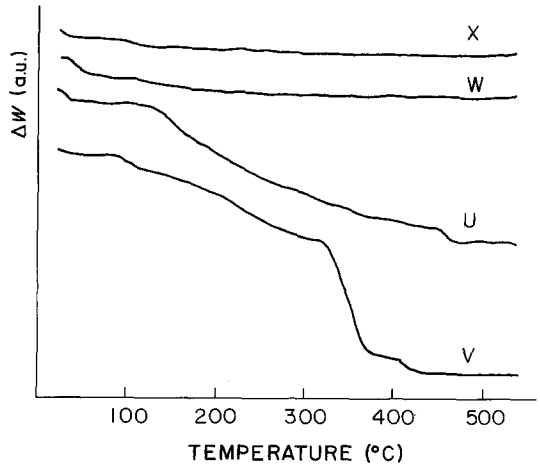

Figure 5 Thermogravimetric analysis runs of Series 2 oxides. For clarity, the curves are displaced vertically (a.u. = arbitrary units).

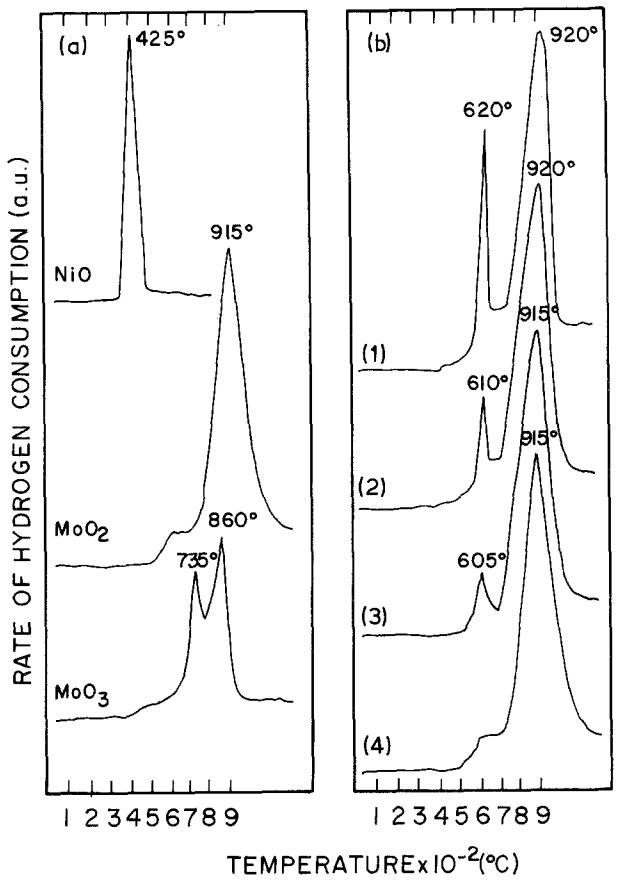

Figure 6 (a) Temperature-programmed reduction spectra of oxides used as standards. (b) Effect of pretreatments of aged MoO_2 on its TPR spectra: (1) none; (2) helium, 700° C, 5 min; (3) helium, 700° C, 15 min; (4) helium, 850° C, 5 min.

3.3.3. Samples from r = 0.30 to 0.55

Within this composition range, the TPR patterns of Series 1 oxides show a gradual growth of two peaks and a diminution of the other two with increasing nickel content. XRD data (Fig. 1) suggest that an increase of α-$NiMoO_4$ content and a decrease of MoO_3 occur with increasing r. Thus, we assign the peaks at about 500 and 700° C to $NiMoO_4$, and the signals at approximately 630 and 750° C to MoO_3. The latter two peaks show T_m values definitely lower than bulk MoO_3, and the first of these coincides with the lower T_m peak of aged MoO_2 samples. This could also be due to decreases in the diffusional constraints that lower the T_m of the peaks of MoO_3.

Sample D, which has the composition most similar to pure $NiMoO_4$ in Series 1, presents only two peaks at 475 and 700° C. The first is very broad, and shows considerable asymmetry in the low T_m side. The 10% excess of nickel over molybdenum in this sample, and the previous data of Sanders and Pratt [10] suggest the presence of highly dispersed NiO, whose T_m is indeed low (about 420° C, Fig. 7b), therefore explaining the observed broadness and asymmetry of the first peak.

The observation of similar TPR patterns in the case of all the nickel molybdate-containing samples, regardless of the specific type of phase (Figs 7a and c), suggests a similar mechanism of reduction for this kind of material. It has been reported that both anhydrous [21–23] and hydrated [3] phases reduce at fairly low temperatures (250 to 400° C), with the formation of metals (nickel, Ni–Mo alloys or inter-

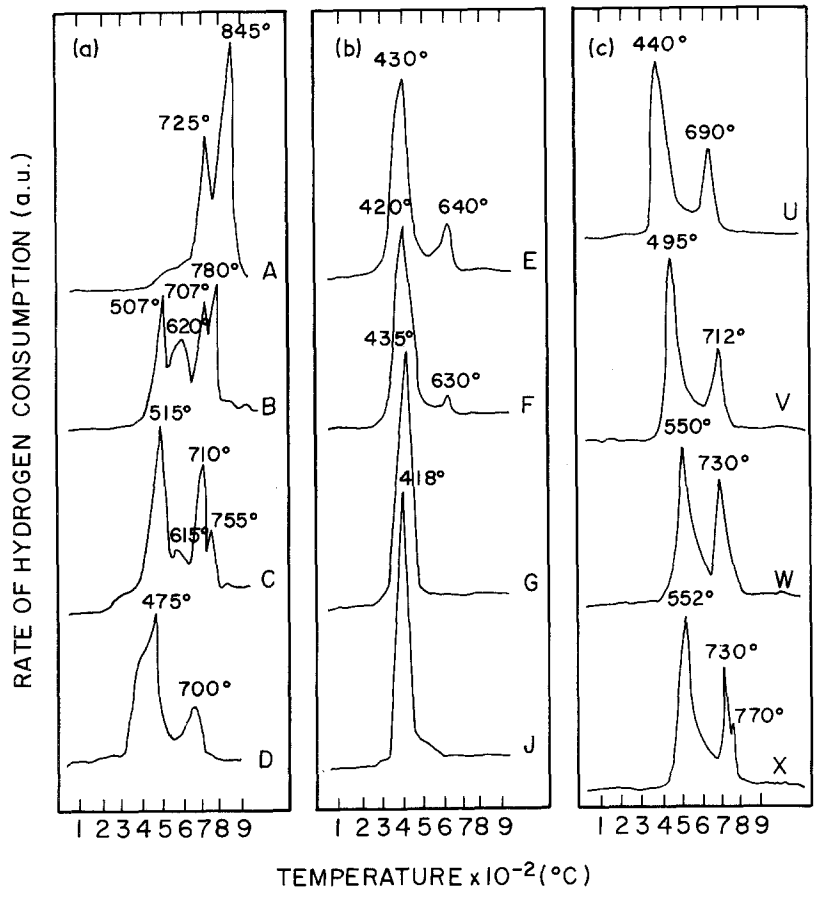

Figure 7 Temperature-programmed reduction spectra of co-precipitated Ni–Mo oxides. (a, b) Series 1; (c) Series 2.

metallics such as $MoNi_4$), plus MoO_2. According to this picture, the low T_m peak may be assigned to the reduction of all the Ni^{2+} and part of the Mo^{6+} to the metallic state, and of the remaining Mo^{6+} to Mo^{4+}. The latter would give rise to the second TPR peak.

In comparing the T_m values of the peaks of Series 2 samples, it may be concluded that the hydrated samples are more easily reduced than the anhydrous ones (Fig. 7c). Additionally, the ratios of the first to the second signals are larger for the hydrated samples, suggesting that more molybdenum is reduced in the first step (Table II). These suggestions agree with a previous report by Astier *et al.* [3], who found that the hydrated nickel molybdate is more reducible than the anhydrous phase. Also, Laine and Pratt [8] found that $NiMoO_4 \cdot H_2O$ is both easier to sulphide and to a higher extent that the anhydrous oxides. Note, however, that Sample D of Series 1 shows an even higher ratio of these peaks, and a very low T_m. This may be accounted by the excess Ni^{2+} present in this sample: it not only would reduce at low temperature but, after being reduced to metallic nickel, it could activate molecular hydrogen, thus promoting the reduction of Mo^{6+}. A similar promotion of the reduction of MoO_3 impregnated with cobalt was observed by Zabala *et al.* [24].

3.3.4. Samples with r > 0.55

As indicated above, molybdenum has only a minor influence on the TPR diagrams of samples within this composition range. This may be explained by assuming a very high dispersion of the molybdenum-bearing oxides plus an intimate contact with the NiO phase. Plyasova *et al.* [13] suggested that solid solutions form in this range of composition of Ni–Mo oxides, but Sanders and Pratt [10], from microscopy observation, concluded that NiO cannot tolerate molybdenum in solid solution. Alternatively they suggested that molybdenum is homogeneously distributed on a very fine scale, which prevented its resolution by electron diffraction. The assumption of an intimate contact of this molybdenum oxide and NiO is necessary, however, as dispersion alone appears unable to lower the T_m of the first peak of Mo^{6+} reduction under 605° C (Fig. 6b). When present in this form, molybdenum oxides are easily reduced along with the NiO, probably due to the activator effect of metallic nickel on H_2.

It is interesting to note that stoichiometric NiO and MoO_3 as well as other Ni^{2+} Mo^{6+} oxides all have clear colours; instead, non-stoichiometric NiO (with either oxygen in excess or a fraction of Ni^{3+} cation) is black [25]. Accordingly, Sample J, which was black just after preparation, turned clear after long-term storage, probably due to loss of the oxygen in excess. On the other hand Samples E, F and G remain black, which may be explained by assuming that dispersed molybdenum oxide provides the oxygen in excess to give the NiO-like phase its black colour. This observation reinforces the view that molybdenum oxides are both highly dispersed and in intimate contact with NiO.

3.4. Relationship between reducibility and HDS activity

The HDS activity of Series 1 sulphided samples has been previously reported [9], and linking to the structure of the sulphide was discussed [10]. It was shown that the most active catalysts (i.e. Samples D and E) consisted mainly of highly dispersed "books" of MoS_2 sheets with very similar structures, although they were generated from very different oxidic forms as discussed above. Samples with a high molybdenum content, on the other hand, showed the presence of MoO_2 whose morphological features suggested that it originated from the excess MoO_3. The common feature between the two most active samples is the very intimate coexistence of nickel and molybdenum in the oxidic phases. Additionally most of the Mo^{6+} present can be easily reduced to neutral molybdenum atoms. In the case of Series 2 samples, the higher reducibility of the $NiMoO_4 \cdot xH_2O$ phase – if compared with $xNiO \cdot MoO_3 \cdot yH_2O$ and α-$NiMoO_4$ – also correlates well with its higher degree of sulphiding and HDS activity as previously reported [8].

In agreement with these observations, Arnoldy *et al.* [26] have proposed a sulphiding mechanism of MoO_3 through the formation of molybdenum metal (i.e. $MoO_3 \rightarrow MoO_2 \rightarrow Mo \rightarrow MoS_2$) that could be operative at temperatures below 680° C. Sulphiding of bulk MoO_2 at low temperatures, in addition to being excessively slow, seems to be limited to a few surface layers [10]. Thus, it appears that easier reduction of Mo^{6+} to neutral molybdenum leads to a higher sulphiding of the samples.

In the case of the alumina-supported catalysts, Ni–Mo formulations were demonstrated to be easier to reduce than the Mo–Al_2O_3 non-promoted ones [7]. Therefore, in these systems where bulk phases have conclusively proved to be not present [12], nickel may play a similar role as in the present unsupported solids, making easier the proper sulphiding of the supported molybdenum oxides.

4. Conclusions

1. TPR has been proved to be a fast (and inexpensive) screening technique to complement other instrumental analysis techniques (e.g. XRD) for the identification of solid-reducible samples.

2. TPR profiles agree with mechanistic proposals regarding the reduction of bulk MoO_3, MoO_2, $NiMoO_4$ and NiO. Physical effects such as variation in the crystal size of MoO_3 or the porosity of MoO_2 led to variations of peak temperature in the spectra. On the other hand, chemical effects such as the interaction of nickel and molybdenum in $NiMoO_4$, gave rise to the appearance of new signals.

3. The higher extent of sulphiding and higher catalytic activity of some samples seem to correlate well with their easier reducibility as determined by TPR.

Acknowledgements

The authors wish to thank Oswaldo Carías, Alberto Albornoz and Francisco Severino for assistance in XRD and SEM analyses. One of us (J.L.B.) gratefully acknowledges a grant from Consejo Nacional de Investigaciones Científicas y Tecnológicas.

References

1. C. H. BARTHOLOMEW and R. W. FOWLER, in Proceedings of 3rd International Conference on the Chemistry and Uses of Molybdenum, edited by H. F. Barry and P. C. H. Mitchell (Climax Molybdenum Co., Ann Arbor, Michigan, 1979) p. 213.
2. C. MAZZOCCHIA, F. DI RENZO, P. CENTOLA and R. DEL ROSSO, in Proceedings of 4th International Conference on the Chemistry and Uses of Molybdenum, edited by H. F. Barry and P. C. H. Mitchell (Climax Molybdenum Co., Ann Arbor, Michigan, 1982) p. 406.
3. M. P. ASTIER, M. L. LACROIX and S. J. TEICHNER, *J. Catal.* **91** (1985) 356.
4. B. C. GATES, J. R. KATZER and G. C. A. SCHUIT, "Chemistry of Catalytic Processes" (McGraw-Hill, New York, 1979) pp. 390–447.
5. N. W. HURST, S. J. GENTRY, A. JONES and B. D. McNICOL, *Catal. Rev.–Sci. Eng.* **24** (1982) 233.
6. D. C. PUXLEY, I. J. KITCHENER, C. KOMODROMOS and N. D. PARKINS, in "Preparation of Catalysts III", edited by G. Poncelet, P. Grange and P. A. Jacobs (Elsevier, Amsterdam, 1983) p. 237.
7. J. BRITO and J. LAINE, *Polyhedron* **5** (1986) 179.
8. J. LAINE and K. C. PRATT, *React. Kinet. Catal. Lett.* **10** (1979) 207.
9. K. C. PRATT, J. V. SANDERS and N. TAMP, *J. Catal.* **66** (1980) 82.
10. J. V. SANDERS and K. C. PRATT, *ibid.* **67** (1981) 331.
11. F. CORBET, R. STEFANI, J. C. MERLIN and C. EYRAUD, *C. R. Acad. Sci.* **246** (1958) 1696.
12. J. LAINE and K. C. PRATT, *Ind. Eng. Chem. Fund.* **20** (1981) 1.
13. L. M. PLYASOVA, I. Yu. IVANCHENKO, M. M. ANDRUSHKEVICH, R. A. BUYANOV, I. Sh. ITENBERG, G. A. KHRAMOVA, L. G. KARAKCHIEV, G. N. KUSTOVA, G. A. STEPANOV, A. L. TSAILINGOL'D and F. S. PILIPENKO, *Kinet. Katal.* (English translation) **14** (1973) 882.
14. K. BRUCKMAN, R. GRABOWSKI, J. HABER, A. MAZURKIEWICZ, J. SLOCZYNSKI and T. WILTOWSKI, *J. Catal.* **104** (1987) 71.
15. R. BURCH, *J. Chem. Soc., Faraday Trans. I* **74** (1978) 2982.
16. P. ARNOLDY, J. C. M. DE JONGE and J. A. MOULIJN, *J. Phys. Chem.* **89** (1985) 4517.
17. R. THOMAS, V. H. J. DE BEER and J. A. MOULIJN, *Bull. Soc. Chim. Belg.* **90** (1981) 1349.
18. A. UENO, Y. KOTERA, S. OKUDA and C. O. BENNET, in Proceedings of 4th International Conference on the Chemistry and Uses of Molybdenum, edited by H. F. Barry and P. C. H. Mitchell (Climax Molybdenum Co., Ann Arbor, Michigan, 1982) p. 250.
19. J. HABER, *J. Less-Common Metals* **54** (1977) 243.
20. F. A. COTTON and G. WILKINSON, "Advanced Inorganic Chemistry", 3rd Edn (Interscience, New York, 1972) p. 548.
21. M. A. KIPNIS and D. AGIEVSKII, *Kinet. Katal.* (English translation) **22** (1981) 1252.
22. A. A. SLINKIN, T. N. KUCHEROVA, G. A. ASHAVSKAYA and T. K. LAVROVSKAYA, *ibid.* **25** (1984) 1032.
23. A. I. VAGIN, N. V. BURMISTROVA and V. I. EROFEEV, *React. Kinet. Catal. Lett.* **28** (1985) 47.
24. J. M. ZABALA, P. GRANGE and B. DELMON, *C. R. Acad. Sci. Ser. C* **279** (1974) 561.
25. A. F. WELLS, "Structural Inorganic Chemistry", 5th Edn (Oxford University Press, Oxford, 1984) p. 538.
26. P. ARNOLDY, J. A. M. VAN DEN HEIJKANT, G. D. DE BOCK and J. A. MOULIJN, *J. Catal.* **92** (1985) 35.

Received 15 December 1987
and accepted 6 May 1988